VILNIUS TECH
Vilnius Gediminas Technical University

Journal of Environmental Engineering and Landscape Management
ISSN 1648–6897 / eISSN 1822-4199
2022 Volume 30 Issue 2: 331–341
https://doi.org/10.3846/jeelm.2022.16764

Special issue on *Sustainable Environmental Processes and Technologies*

COLUMN STUDY FOR THE CU(II) REMOVAL BY THE COCONUT SHELL FROM AQUEOUS SOLUTION – MLR AND GA MODELING

Shreyashi SARKAR[1], Nirjhar BAR[1, 2], Sudip Kumar DAS[1*]

[1]*Chemical Engineering Department, University of Calcutta, 92, A. P. C. Road, 700009 Kolkata, West Bengal, India*
[2]*St. James' School, 165, A. J. C. Bose Road, 700014 Kolkata, West Bengal, India*

Received 15 January 2021; accepted 21 December 2021

Highlights

- Copper removal by continuous column operation using inexpensive adsorbent.
- Process parameters like flow rate, bed height, and metal ion concentration are optimized.
- Kinetic models such as Yoon-Nelson, Thomas, Adams-Bohart, Wolborska, Yan et al. were applied to the experimental data to find out the packed bed capacity.
- MLR and GA modeling are applied successfully.

Abstract. Adsorption characteristics of locally available inexpensive natural adsorbent coconut shells were studied for Cu(II) removal. The present study adsorption process was carried through a fixed bed column to find out the breakthrough characteristics. The variation of operating variables is investigated, pH 6, influence Cu(II) concentration (10–30 mg·L^{-1}), bed height (5–15 cm), the flow rate (10–30 ml·min^{-1}). The suitability of various kinetic models has been tested. Maximum adsorption capacity, q_e according to Thomas model, was 30.09 mg·g^{-1}obtained at 20 ml/min, flow rate, 30 mg·L^{-1} metal solution, and 15 cm bed height. The correlation coefficient of the Thomas model ranges from 0.8260 to 0.9839. Besides this, according to the statistical parameters of the Yoon-Nelson and Yan et al. models, proving that the experimental data are suitable for this model. The statistical and GA modeling of the experimental data has also been performed successfully.

Keywords: adsorption, Cu(II) removal, column operation, Multiple Linear Regression, Genetic Algorithm.

Introduction

Rapid industrialization continuously releases large quantities of heavy metals released in water bodies. Cadmium, copper, zinc, lead, nickel, mercury, and chromium are released in water from mining, metal plating, battery manufacture, tanneries, paint manufacturing industries, etc. (Ngah & Hanafiah, 2008). Copper is an essential micronutrient for the human body, plants, and microorganisms. Excessive copper concentration in human bodies causes different diseases such as kidney damage, anemia, and gastrointestinal problems. In drinking water and industrial effluent, copper permitted value is 1.5 and 3 mg·L^{-1}, respectively (Bureau of Indian Standards, 2012). Different techniques like electrochemical precipitation, ion exchange, membrane separation, reverses osmosis, ultrafiltration, and adsorption can be used to treat industrial wastewater (Singha & Das, 2013). However, the adsorption process effectively replaces the costly wastewater treatment process among these technologies. Inexpensive agricultural wastes are readily available and can be utilized for metal removal.

More than 140 million metric tons of agricultural waste materials are generated worldwide (Galo-Cordova et al., 2017). Agrarian waste material is used Cu(II) removal in this study. A variety of processes accumulates a substantial amount of metals. The advantages of these materials as adsorbents are good adsorptive removal efficiency and cost-effectiveness. The metal uptake involves adsorption, diffusion, complexation, chelation, and coordination, depending on the adsorbent surface's nature (Pino et al., 2006; Kuyucak & Volesky, 1988; Esposito et al., 2001; Pino, 2005; Arena et al., 2016). The literature review suggested that agricultural waste has been extensively tried to remove aqueous solutions (Arena et al.,

*Corresponding author. E-mails: *drsudipkdas@gmail.com; skdchemengg@caluniv.ac.in*

2016; Singha & Das, 2011; Sarkar & Das, 2016b). Here, the coconut shell was used for copper removal.

The coconut shell consists of lignin (33.30 wt%), cellulose (30.58 wt%), hemicellulose (26.70 wt%), water (8.86 wt%), and ash (0.56 wt%) (Arena et al., 2016). This material is water-insoluble, chemically stable, and has good mechanical strength. The experimental investigation reported using coconut shell powder, i.e., *Cocosnucifera*, as an adsorbent in fixed-bed.

Statistical analysis of the data is essential, and the approach of analysis of data to extract hidden information using machine learning has also become popular in the recent past (Nag et al., 2020; Das et al., 2019; Mandal et al., 2020; Ghosh et al., 2021; Nag et al., 2019). In this regard, the use of MLR (multiple linear regression) has been used by researchers in the recent past.

Using the genetic algorithm for modeling purposes has also become highly fruitful for analyzing data and extracting information (Nag et al., 2019, 2020; Das et al., 2019; Mandal et al., 2020; Ghosh et al., 2021; Mitra et al., 2019). The prediction of percentage removal can be made using GA to validate the data.

1. Experimental

1.1. Bioadsorbent preparation

The coconut shell was used as the bio-sorbent. After collection, it was crushed and ground. 0.1 N NaOH and 0.1 N H_2SO_4 were used to remove the colour materials (Singha & Das, 2011; Sarkar & Das, 2016). Then after washing with distilled water, it was dehydrated at 105 °C for 6 hours. Finally, the coconut shell was sieved to get a particle size amounting to –44+52 mesh size (250 to 350 μm). Then it is stored in a desiccator.

1.2. Metal solution preparation

3.929 gm of copper(II) sulphate pentahydrate was used to prepare a copper stock solution of concentration 1000 mg·L^{-1}. Different copper(II) solution was prepared from standard solution (Sarkas & Das, 2016).

1.3. Instrument and reagents used

The reagents were used in analytical grade from Merck India. The instruments used were (1) WTW pH meter (Multi 340i/SET, Germany), (2) the BET analyzer (Quanta Chrome, USA), ASS (Model - AA 240 VARIAN, Australia), FTIR (Nicolet^{TM}5N, Thermo Fisher, USA).

1.4. Biosorption experiments

The column diameter was 2 cm, and a height of 50 cm was used for the experiment. The desired amount of adsorbent was placed in glass columns. A peristaltic pump (Model-7535-04, Cole-Parmer, USA), pumped the desired concentration of the metal solution to the column from the top. Cu(II) ion in water samples was measured using atomic absorption spectrophotometer. Figure 1 shows the experimental setup.

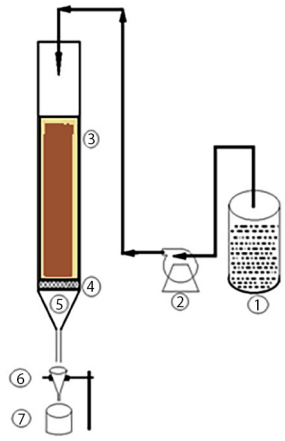

Figure 1. Schematic diagram of experimental set up of column study: 1 – Reservoir tank with metal solution; 2 – Peristaltic pumps; 3 – Porous bed; 4 – Glass beads; 5 – Conical outlet section; 6 – Filter; 7 – Treated effluent storage

2. Results and discussion

The BET surface area is 0.52 m^2/g and the point of zero charge is 6.62. The point of zero charge has been determined by the solid addition method (Singha & Das, 2011).

The coconut shell surface is a highly irregular, porous, and heterogeneous structure with fibrous texture shown in the SME (Figure 2).

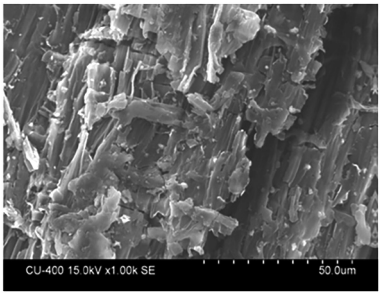

Figure 2. Scanning electron microghaph (SEM) of coconut shell

The pH variation in the 2–7 was studied in batch experiments and shown in Figure 3. All of the investigations have been carried out three times to confirm the reproducibility of the experimental results. This reproducibility and the relative deviation have been measured as ±0.5% and ±2.5%, respectively. Copper is found to be present in different forms at different pH solutions. Cu^{2+} and $Cu(OH)^+$ are the main forms at pH range of 2–6. The hydronium ions are predominant at the low pH. Therefore, copper(II) ions compete with H_3O^+ ions to capture the coconut shell's useful adsorption site. With the increase of pH value starting from 2 up to 6, the Cu(II) adsorption is increased due to the electrostatic attraction between the surface of the adsorbent and the Cu(II) ion. At pH > pH_{PZC}, the coconut

shell's surface becomes negative, promoting the Cu(II) adsorption. At pH > 6 there is a possibility of precipitation of $Cu(OH)_2$. At lower pH the $Cu(OH)_2$ is found to be more soluble than higher pH. Hence the optimum value of pH is 6 (Singha & Das, 2013; Ahmad et al., 2012). So, all experiments in a column study are carried out at pH 6. As the solution pH increases, the functional groups containing oxygen become deprotonated and enhance the electrostatic attraction. Then after the adsorption, the pH of the solution varies from 6 to 6.11.

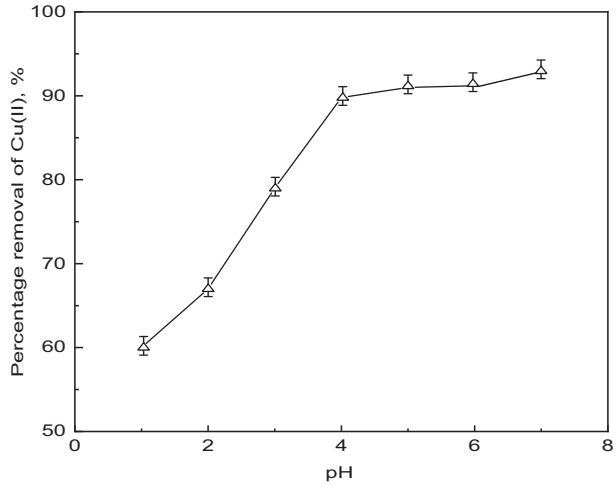

Figure 3. Variation of pH on the Cu(II) adsorption: Initial Cu(II) concentration: 25 mg/L; Adsorbent dose: 10 g/L; Contact time: 5 h

2.1. Flow rate variation

Figure 4 shows the breakthrough curve. The breakthrough curves were steeper with a faster flow rate. The breakthrough time increased as the flow rate decreased, and the copper solution got more time for the adsorption. This phenomenon increased the breakthrough time at the lower flow rate, leading to the maximum Cu(II) removal. Other researchers also found similar results (Mitra et al., 2021; Sivaprakash et al., 2010).

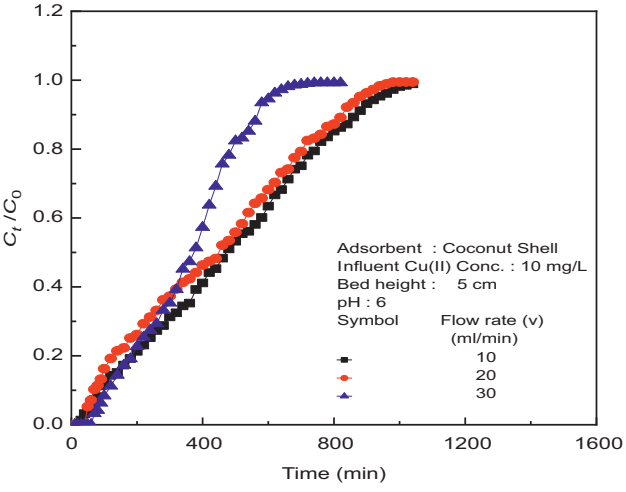

Figure 4. Effect of flow rate for Cu(II) adsorption on coconut shell at constant bed height and influent metal ion concentration

2.2. Influence of metal ions concentration

Figure 5 shows the breakthrough curve. The breakthrough curves are found to be steeper at higher concentrations. From this graph, it was clear that the breakthrough time decreased as the ion's influent concentration increased. Hence, the adsorption rate reduced with the rising metal ion concentration because higher metal ions were present at the limited adsorption sites. Due to this, saturation occurred more quickly than the lower metal ion concentration. The adsorption capacity was maximum at low metal ion concentration. Other researchers also found similar results. Similar observations are obtained by other researchers (Deepali, 2011).

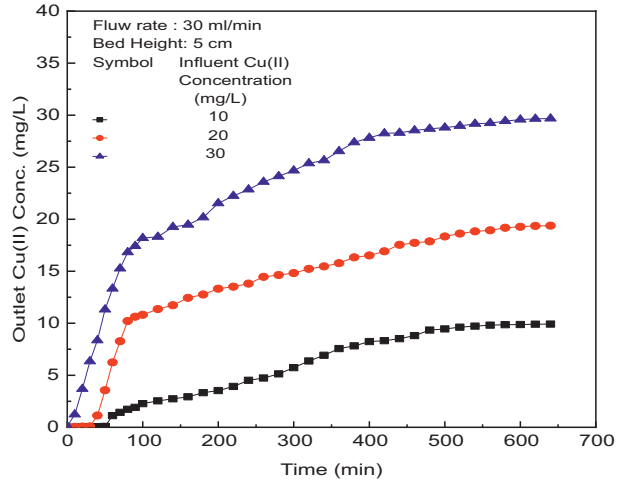

Figure 5. Effect of influent metal ions concentration for the removal of Cu(II) on coconut shell at constant bed height and flow rate

2.3. Influence of packing height

The removal process depended on the packed bed's height, and breakthrough time varied with packing height (Figure 6). The breakthrough curves were sharper with lower bed height. The adsorbent saturation took a much longer time

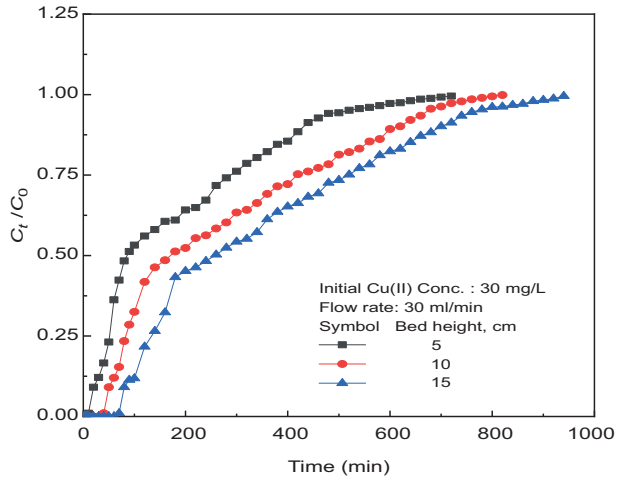

Figure 6. Effect of bed height of column for removal of Cu(II) on coconut shell constant flow rate and influent metal ion concentration

as the packing height increased, and the metal solution got much more contact with the active sites in the bed. The maximum metal removal occurred at 15 cm bed height. At lower bed height, the amount of metal removal was lower than the higher packing height because, at lower packing height, metal solution got less adsorbent than the higher bed height. Other researchers also found similar results (Hasfalina et al., 2012; Nwabanne & Igbokwa, 2012).

2.4. Kinetic modeling

The equation of maximum adsorption capacity is as follows:

$$q_e = \frac{v}{1000w}\int_0^{t_{total}} (C_0 - C_t)dt; \quad (1)$$

$$q_{e\max} = \frac{q_{total}}{w}. \quad (2)$$

2.4.1. Bohart-Adams model (Bohart & Adams, 1920)

It is based on surface reaction theory and expressed as:

$$\ln\left(\frac{C_t}{C_o}\right) = k_{AB}C_0 t - k_{AB}N_0\left(\frac{z}{v}\right). \quad (3)$$

The value of N_0 and k_{AB} are calculated using $\ln\left(\frac{C_t}{C_0}\right)$ versus t plot. As the flow rate increases, k_{AB} also increases. Table 1 shows the parameters with R^2 that vary in the ranges of 0.5982–0.9907. The rate constant, k_{AB}, increases from 5×10^{-4} ml·min^{-1}·mg^{-1} to 18.1×10^{-4} ml·min^{-1}·mg^{-1} with the increases of the flow rate range from 10–30 ml·min^{-1} for constant bed height and concentration. The saturation concentration N_0 reached a maximum at 20 ml·min^{-1} flow rate.

2.4.2. Yoon-Nelson model (Yoon & Nelson, 1984)

It is expressed as:

$$\frac{C_t}{C_0 - C_t} = \exp(k_{YN}t - k_{YN}\tau). \quad (4)$$

The τ and k_{YN} are found using $\ln\left(\frac{C_t}{C_0 - C_t}\right)$ versus t plot. Table 2 shows the parameters. The breakthrough time, τ decreased, and constant k_{YN} increased with the rise of flow rate. The value of R^2 ranges from 0.6547–0.9891. The breakthrough time, τ, decreases from 444.800 to 217.644 min, and the rate constant, k_{YN}, increases from 0.0207–0.0071 min^{-1} with the rise of the flow rate range from 10–30 ml·min^{-1}.

2.4.3. Thomas model (Thomas, 1944)

It assumes the Langmuir kinetic model is valid with no mass transfer and axial dispersion. It is expressed as:

$$\ln\left(\frac{C_t}{C_0} - 1\right) = \left(\frac{k_{Th}q_e x}{Q}\right) - k_{TH}C_0 t. \quad (5)$$

Table 3 shows the parameters. With the increased flow rate, the q_e decreased, and k_{Th} decreased as the adsorbent dose increased. The range of R^2 varies from 0.8260 to 0.9839. The rate constant, k_{Th} decreases from 0.61–0.11 ml·min^{-1}·mg^{-1} as the adsorbent dose increases. From Table 3 the predicted maximum adsorption capacities, q_0 were much higher than the experimental adsorption capacity. Hence, this model was inappropriate, and due to the rate-limiting step was either external or internal diffusion (Idan et al., 2017).

Table 1. Bohart-Adams model parameters using linear regression analysis

Flow rate, v (ml·min^{-1})	Influent concentration, C_0 (mg·L^{-1})	Bed height (cm)	Rate constant, $k_{AB}\times10^{-4}$ (ml·min^{-1}·mg^{-1})	Saturation concentration, N_0 (g·L^{-1})	R^2
10	10	5	5.00	8.59	0.8063
20	10	5	4.00	15.46	0.8076
30	10	5	18.1	11.72	0.5982
10	20	5	2.00	13.49	0.8413
20	20	5	1.00	38.74	0.8662
30	20	5	3.00	1.87	0.9876
10	30	5	0.50	40.24	0.9084
20	30	5	0.90	47.76	0.9374
30	30	5	1.00	24.07	0.9832
10	30	10	1.00	27.02	0.9451
20	30	10	0.80	36.56	0.9088
30	30	10	1.20	19.37	0.9807
10	30	15	0.80	23.56	0.9703
20	30	15	0.70	28.22	0.8802
30	30	15	1.00	15.02	0.9907

Table 2. Yoon-Nelson model parameters using linear regression analysis

Flow rate, v (ml·min^{-1})	Influent concentration, C_0 (mg·L^{-1})	Bed height (cm)	Time, τ (min)	Rate constant, k_{YN} (min^{-1})	R^2
10	10	5	444.800	0.0071	0.8673
20	10	5	357.968	0.0064	0.7160
30	10	5	217.644	0.0207	0.6547
10	20	5	306.821	0.0070	0.8952
20	20	5	451.337	0.0049	0.9160
30	20	5	81.787	0.0111	0.9948
10	30	5	439.741	0.0026	0.9396
20	30	5	262.659	0.0043	0.9621
30	30	5	41.966	0.0100	0.9881
10	30	10	333.777	0.0035	0.9464
20	30	10	461.971	0.0038	0.9521
30	30	10	85.806	0.0064	0.9754
10	30	15	1288.585	0.0031	0.9753
20	30	15	607.288	0.0030	0.9464
30	30	15	95.514	0.0055	0.9891

Table 3. Thomas model parameters using linear regression analysis

Flow rate, v (ml·min^{-1})	Influent concentration, C_0 (mg·L^{-1})	Bed height (cm)	k_{Th} (ml·min^{-1}·mg^{-1})	$q_{e(\mathrm{cal})}$ (mg·g^{-1})	$q_{e(\mathrm{exp})}$ (mg·g^{-1})	R^2
10	10	5	0.61	7.94	4.44	0.9036
20	10	5	0.57	14.24	7.99	0.8442
30	10	5	1.03	5.51	8.82	0.8260
10	20	5	0.25	12.31	6.77	0.8747
20	20	5	0.22	30.09	16.62	0.9116
30	20	5	0.46	13.13	7.42	0.9620
10	30	5	0.07	29.67	14.93	0.9424
20	30	5	0.12	28.63	16.62	0.9704
30	30	5	0.15	14.34	7.34	0.9452
10	30	10	0.11	22.93	12.27	0.9801
20	30	10	0.12	22.84	12.45	0.9515
30	30	10	0.14	8.33	4.40	0.9412
10	30	15	0.12	16.81	8.98	0.9839
20	30	15	0.10	50.05	9.25	0.9422
30	30	15	0.10	5.01	1.58	0.9215

2.4.4. Wolborska model (Wolborska, 1989)

It is expressed as:

$$\ln\left(\frac{C_t}{C_o}\right) = k_{AB}C_0 t - k_{AB}N_0\left(\frac{z}{v}\right). \quad (6)$$

The external mass transfer coefficient, β, increases with the flow rate value and decreases at higher bed height values. The value of R^2 ranges from 0.5982–0.9907 and is shown in Table 4. The β increased from 0.6290–0.9334 L·min^{-1} as flow rate rises 10–20 ml·min^{-1}. Similarly, saturation concentration is maximum at 20 ml·min^{-1}.

2.4.5. Yan et al. model (Yan et al., 2001)

The model is:

$$\ln\left(\frac{Ct}{C0 - Ct}\right) = \frac{K_Y}{Q}C0\ln\left(\frac{Q^2}{K_Y q_Y m}\right) + \frac{K_Y C0}{Q}\ln t. \quad (7)$$

The q_Y increases at a higher bed height and flow rate. However, K_Y increases only at a higher flow rate. The ranges of correlation coefficient lie between 0.8278–0.9913. Table 5 shows the model parameters. The higher adsorption capacity and the value of the correlation coefficient prove that the model was well fitted. The rate constant,

Table 4. Wolborska model parameters using linear regression analysis

Flow rate, v (ml·min^{-1})	Influent concentration, C_0 (mg·L^{-1})	Bed height (cm)	β (L·min^{-1})	Saturation concentration, N_0 (g·L^{-1})	R^2
10	10	5	0.6290	8.59	0.8063
20	10	5	0.9334	15.46	0.8076
30	10	5	2.6809	11.72	0.5982
10	20	5	0.4447	13.49	0.8413
20	20	5	0.9227	38.74	0.8662
30	20	5	0.7375	1.87	0.9876
10	30	5	0.2819	40.24	0.9084
20	30	5	0.5615	47.76	0.9370
30	30	5	0.5520	24.07	0.9832
10	30	10	0.3575	27.02	0.9451
20	30	10	0.3915	36.56	0.9080
30	30	10	0.2937	19.37	0.9807
10	30	15	0.2652	23.56	0.9703
20	30	15	0.2643	28.22	0.8802
30	30	15	0.1968	15.02	0.9907

K_Y increases 1428.13–7152.06 ml·mg^{-1}·min^{-1} as the flow rate increases. Still, adsorption capacity does not follow any definite pattern, and the maximum value is obtained at 20 ml·min^{-1} for a fixed adsorbent dose.

Based on the correlation coefficient, R^2, the Yan et al. model was suitable to predict the Cu(II) adsorption behavior in fixed-bed.

2.4.6. Bed Depth Service Time (BDST) model

It is a straightforward technique for the relationship between the bed height and service time in which the process concentrations and adsorption are the parameters. Initially, Bohart and Adams (1920) formulated a correlation between bed height and breakthrough time. Later on, Hutchins (1973) linearized this model as:

$$t = \frac{N_0}{C_0 v} z - \frac{1}{k_B C_0} \ln\left(\frac{C_0}{C_t} - 1\right). \quad (8)$$

Equation (8) has a linear form and is represented as:

$$t = mz + b, \quad (9)$$

where:

$$m = \frac{N_0}{C_0 v}; \quad (10)$$

$$b = -\frac{1}{k_B C_0} \ln\left(\frac{C_0}{C_t} - 1\right). \quad (11)$$

Figure 7 shows the plot of service time vs. bed depth at the flow rate of 30 ml·min^{-1} and influent concentration of 30 mg·L^{-1}. The high correlation coefficient magnitude ($R^2 > 0.99$) indicated the suitability of this model for the present adsorption system. The value of k_B and N_0 was evaluated from the plot's intercept and slope (Figure 7) and shown in Table 6. These parameters could be used for the scale-up design of the fixed-bed column.

Table 5. Yan et al. model parameters using linear regression analysis

Flow rate, v (ml·min^{-1})	Influent concentration, C_0 (mg·L^{-1})	Bed height (cm)	Rate constant, k_Y (ml·mg^{-1}·min^{-1})	q_Y (mg·g^{-1})	R^2
10	10	5	1428.13	5.94	0.9778
20	10	5	2093.20	12.57	0.9913
30	10	5	7152.06	4.43	0.8657
10	20	5	399.97	16.74	0.9851
20	20	5	749.32	38.40	0.9745
30	20	5	564.915	28.29	0.9267
10	30	5	124.88	117.51	0.9613
20	30	5	265.02	99.56	0.9335
30	30	5	214.51	32.60	0.9724
10	30	10	355.74	38.82	0.8839
20	30	10	395.10	68.79	0.9518
30	30	10	189.57	50.71	0.8278
10	30	15	343.60	47.41	0.7917
20	30	15	404.00	50.66	0.9677
30	30	15	182.81	44.79	0.8851

Table 6. Regression analysis of service time vs. bed height. Flow rate: 30 ml·min^{-1}; Influent concentration: 30 mg·L^{-1}, $\frac{C_t}{C_0} = 0.1$

Bed height (cm)	Break-through time (min)	Exhaust time (min)	N_0 (g·L^{-1})	k_B (L·mg^{-1}·min^{-1})	Correlation coefficient R^2
5	22.21	683.85	5.42	8.59X10^{-3}	0.9987
10	50.43	783.60			
15	82.43	924.91			

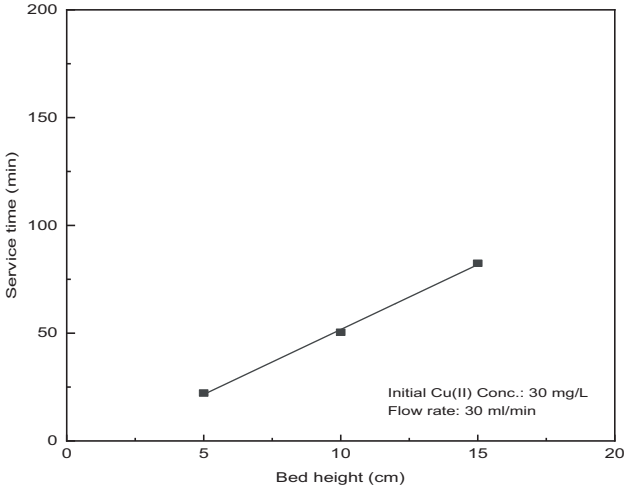

Figure 7. BDST model

2.4.7. MLR modeling

The following equation is evaluated from the experimental data (Table 7) when coconut shell has been used as the adsorbent to measure the removing efficiency of Cu(II):

$$y = 1.068475 - 0.244450 \times x_1 - 1.106807 \times x_2 - 0.202499 \times x_3 + 0.008984 \times x_4. \quad (12)$$

The variance of the estimate, MSE, and correlation coefficient calculated from Eq. (12) are 0.058169, 0.003384, and 0.970538, respectively, with a *t*-value of 1.9702 for 234 degrees of freedom with a 95% confidence range. The comparison of predicted to the experimental values can be seen in Figure 8.

Table 7. Data description for MLR and GA analyses

Independent variable		Range
Adsorbent		Coconut shell
Flow rate (mg/L)	x_1	10 to 30
Contact time (min)	x_2	10 to 1040
Initial concentration (mg/L)	x_3	10 to 30
Effluent concentration (mg/L)	x_4	0 to 29.46
Dependent variable		
Percentage removal	y	0.67 to 100

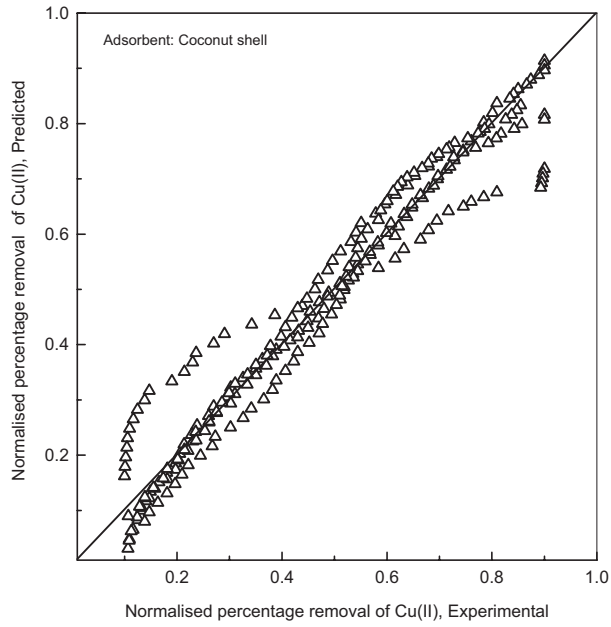

Figure 8. Regression analysis comparison curve with coconut shell as adsorbent

2.4.8. GA modeling

Analyses using genetic algorithm (GA) have provided us with excellent modeling in the past. With this expectation, the present study has been undertaken for modeling. The three different random distribution of the same data has been considered, i.e., RCu_1, RCu_2, and RCu_3 are the three different sets used for the GA analyses separately. This separation of different distributions is expected to eliminate all possibilities of random error. The roulette selection rule, the probability of crossing over, and the mutation of 0.9 and 0.1, respectively, have produced the best network architecture. Figure 9 presents the errors concerning the

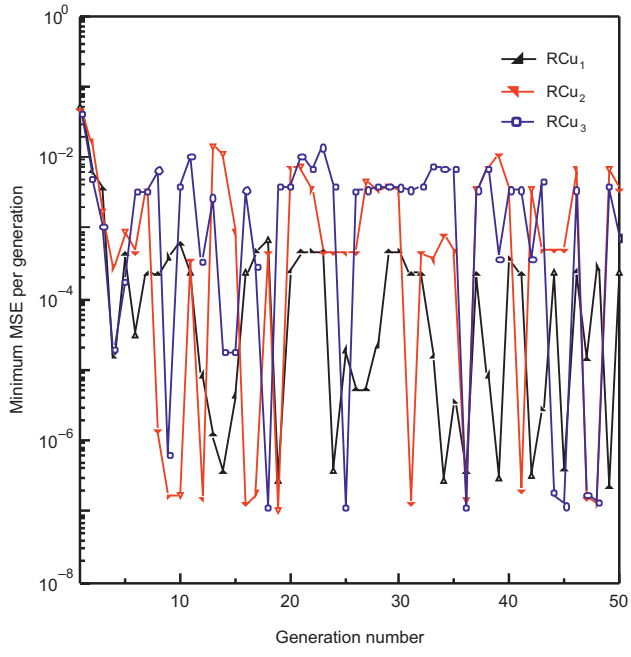

Figure 9. Variation of generation number

various, i.e., 50 generation numbers. The generation with the least error is considered for the final prediction.

Along with the generation number, the value of population size has also been kept at 50. From Figure 10 it can be ascertained that the performance is excellent. The numbers concerning the error and the excellent correlation coefficient value from Table 8 also reiterate this fact. So, it can be said that GA has been applied successfully for the present study for modeling.

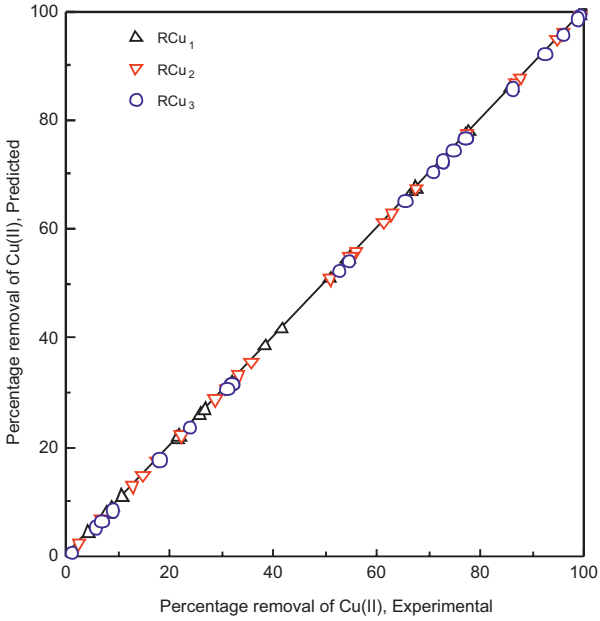

Figure 10. Final comparison related to GA prediction

3. Disposal of the metal-loaded adsorbent

Initially, at 700 °C, the loaded adsorbents are burned for 1 h. 5 mg of the ash sample is mixed in deionized water with a volume of 25 ml to have a solid-liquid ratio of 1:5 (Liu & Sun, 2012; Senthil et al., 2015). After 24 h of repeated stirring, the filtrate was tested for Cu(II) ions. It was seen that Cu(II) ions did not come out from the given ash sample.

4. Desorption studies

The desorption study was carried out using Concentrated HCl (1–6 N). Figure 11 shows the regeneration graph, and as the strength of HCl increases, the regeneration capability of the adsorbent increases (Singha & Das, 2013). The regeneration process continued up to the second cycle, and adsorption efficiency decreased rapidly after the 2nd cycle.

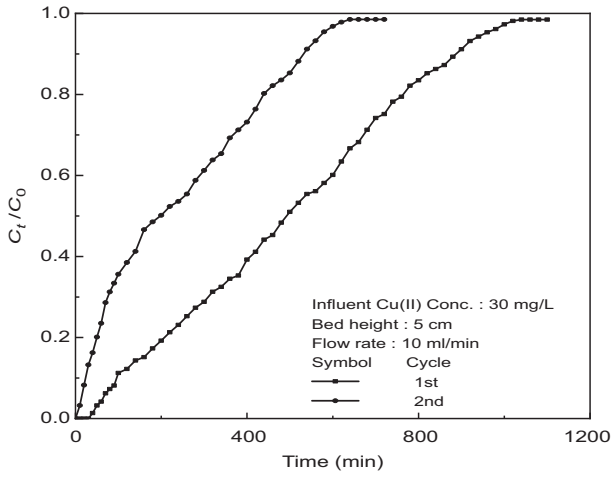

Figure 11. Regeneration plot with experimental data for the adsorption of Cu(II) on coconut shell

5. FTIR study

Figure 12 represents the FTIR spectra of Cu(II) loaded and fresh coconut shells. The band shifted around the peak 3430 cm^{-1} shows the involvement of –OH group. The peak around 2910 cm^{-1} is for –CH stretching in –CH, $–CH_2$, and $–CH_3$ groups. The bands at around 1740 and 1255 cm^{-1} indicate the C=C bonds in aromatic rings. The presence of C–O carboxyl bands at 1635 and 1250 cm^{-1}. The 1597 and 1505 cm^{-1} peaks represent the conjugate C–O group in the aromatic ring for lignin and 1460 cm^{-1} peak for –C–H in lignin. 1422 cm^{-1} band is due to $–CH_2$ deformation in cellulose or the –C–H deformation in the lignin. 950 to 1100 cm^{-1} peaks indicate C–H group's presence in cellulose, and the 1237 cm^{-1} is for C–O group

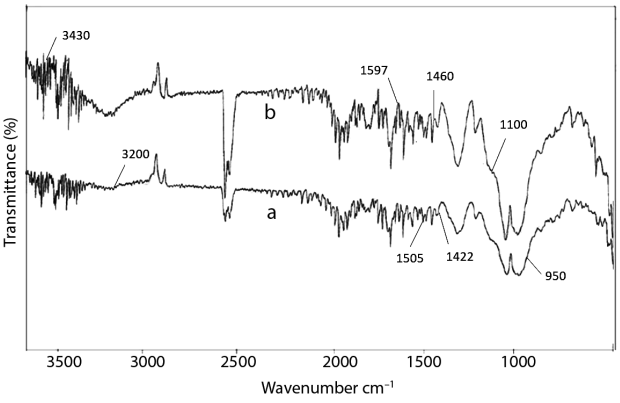

Figure 12. FTIR spectra of (a) coconut shell and (b) Cu(II) loaded coconut shell

Table 8. Performance of the optimized GA network

Randomisation No.	Minimum MSE of cross-validation	AARE	SD (σ)	MSE	CCC (R)
RCu_1	1.1964×10^{-7}	0.000853	0.001781	0.000696	1
RCu_2	9.6785×10^{-8}	0.000892	0.001834	0.001280	0.999999
RCu_3	1.0149×10^{-7}	0.005152	0.022379	0.000740	1

from the acetyl group in the lignin. 1610 cm^{-1} peak represents the C–O–C group from cellulose and hemicellulose. The band 1370 cm^{-1} is for C–H deformation in the cellulose as well as in the hemicellulose. The observed peak at 1035 cm^{-1} represents Si–O stretching and bending, indicating silica. Due to the N–H group, the peak at 3430 cm^{-1} shifted to around 3200 cm^{-1} in the metal-loaded coconut shell.

6. Comparison study of copper adsorption between different adsorbents

A comparison study based on the adsorptive capacities of the adsorbents was also reported. The maximum capacity for adsorption as per the Thomas model was compared and represented in Table 9. The adsorptive capacity of an adsorbent is dependent on its characteristics. It changes with various process conditions. The Physical characterization of coconut shells reveals that coconut shells have many metal-binding groups and a high surface area. These are very suitable for Cu(II) adsorption. The capacity of adsorption of the coconut shell was excellent when it was compared with the other adsorbents.

Table 9. Different capacities of Cu(II) removal by several adsorbents previously reported by other researchers

Adsorbents	Thomas maximum adsorption capacity ($mg \cdot g^{-1}$)	References
Functionalized SBA-1 mesoporous silica with polyamidomines	101.68	Shahbazi et al. (2013)
Kenaf (*Hibiscus Cannabius, L)* fibers	42.27	Liu and Sun (2012)
Polyaniline-coated saw dust	58.23	Senthil et al. (2015)
Surface modified eucalyptus globulus seeds	300.5	Kapur and Mondal (2016)
Magnetized saw dust (Fe_2O_3-SD)	43.45	Kapur and Mondal (2016)
Amino functionilized ramie stalk	33.55	Wang et al. (2018)
Sugar cane baggasse	67.36	Xavier et al. (2018)
Rice Husk Ash	3.07–10.77	Sarkar and Das (2016a)
Activated neem bark	12.45	Maheshwari and Gupta (2016)
Tetraethylenepentamine modified sugar cane bagasse	16.52	Chen et al. (2017)
Rice husk based carbon	36.41	Yahaya et al. (2011)
Free algae *Sargassum sp.*	96.32	Barquilha et al. (2017)
Immobilized algae *Sargassum sp.*	130.91	Barquilha et al. (2017)
Peanut shell	30.67	Banerjee et al. (2019b)
Almond shell	12.96	Banerjee et al. (2019b)
Pistochio shell	33.64	Banerjee et al. (2019a)
Guava leaves	49.04	Mitra and Das (2020)
Hyacinth root	16.62	Mitra and Das (2020)
Coconut shell	5.01–30.09	Present study

Conclusions

The fixed-bed experiments were performed using coconut shells as adsorbents. The optimal Cu(II) removal adsorption was obtained at 20 $ml \cdot min^{-1}$, flow rate, 30 $mg \cdot L^{-1}$ metal solution, and 15 cm bed height. The breakthrough curves were analyzed by using different kinetic models. The Thomas, Yoon-Nelson, and Yan et al. models were well fitted for the data for predicting the breakthrough curves. However, Yan et al. model had been the most suitable. Maximum adsorption capacity, q_e according to Thomas model, was 30.09 $mg \cdot g^{-1}$ obtained at 20 ml/min, flow rate, 30 $mg \cdot L^{-1}$ metal solution, and 15 cm bed height. The Thomas maximum adsorption capacity was compared with the literature value. MLR and GA modeling has been successfully performed by analyzing the experimental data. The coconut shell can be an excellent green adsorbent related to the adsorption of Cu(II). It can also be used and applied in small and medium-sized industries in 3rd World countries.

Acknowledgements

S. Sarkar is thankful to UGC, Govt. of India, New Delhi (F1-17.1/2012-13/RGNF-2012-13-SC-WES-24757/(SA-III/Website) dt. 6.6.12) for the research fellowship.

Nomenclature

C_0 initial Cu(II) concentration ($mg \cdot L^{-1}$)
C_t Cu(II) concentration at time t ($mg \cdot L^{-1}$)
k_B adsorption rate constant in BDST model ($L \cdot min^{-1} \cdot mg^{-1}$)
k_{AB} kinetic constant ($ml \cdot min^{-1} \cdot mg^{-1}$)
k_{Th} rate constant ($ml \cdot min^{-1} \cdot mg^{-1}$)
k_{YN} rate constant (min^{-1})
k_Y rate constant ($ml \cdot mg^{-1} \cdot min^{-1}$)
m mass of the adsorbent (g)
N_0 adsorption capacity ($g \cdot L^{-1}$)
q_e Thomas maximum adsorption capacity ($mg \cdot g^{-1}$)
x mass of the adsorbent (g)
Q flow rate of metal solution ($ml \cdot min^{-1}$)
t breakthrough time (min)
v flow rate of metal solution ($ml \cdot min^{-1}$)
z bed depth (cm)

Greek letters

β Wolborska model constant ($L \cdot min^{-1}$)
τ time required for 50% adsorbate breakthrough (min)

References

Ahmad, R., Kumar, R., & Haseeb, S. (2012). Adsorption of Cu^{2+} from aqueous solution onto iron oxide coated eggshell powder: Evaluation of equilibrium, isotherms, kinetics, and regeneration capacity. *Arabian Journal of Chemistry*, *5*(3), 353–359. https://doi.org/10.1016/j.arabjc.2010.09.003

Arena, N., Lee, J., & Clift, R. (2016). Life Cycle Assessment of activated carbon production from coconut shells. *Journal of Cleaner Production*, *125*, 68–77. https://doi.org/10.1016/j.jclepro.2016.03.073

Banerjee, M., Basu, R. K., & Das, S. K. (2019a). Adsorptive removal of Cu(II) by pistachio shell: Isotherm study, kinetic modelling and scale-up designing – continuous mode. *Environmental Technology & Innovation*, *15*, 100419. https://doi.org/10.1016/j.eti.2019.100419

Banerjee, M., Basu, R. K., & Das, S. K. (2019b). Cu(II) removal using green adsorbents: Kinetic modeling and plant scale-up design. *Environmental Science and Pollution Research*, *26*, 11542–11557. https://doi.org/10.1007/s11356-018-1930-5

Barquilha, C. E. R., Cossich, E. S., Tavares, C. R. G., & Silva, E. A. (2017). Biosorption of nickel(II) and copper(II) ions in batch and fixed-bed columns by free and immobilized marine algae *Sargassum* sp. *Journal of Cleaner Production*, *150*, 58–64. https://doi.org/10.1016/j.jclepro.2017.02.199

Bohart, G. S., & Adams, E. Q. (1920). Some aspects of the behavior of charcoal with respect to chlorine. *Journal of the American Chemical Society*, *42*, 523–544. https://doi.org/10.1021/ja01448a018

Bureau of Indian Standards. (2012). *Indian standard drinking water – specification* (IS 10500:2012, 2nd ed.). http://cgwb.gov.in/Documents/WQ-standards.pdf

Chen, J.-D., Yu, J.-X., Wang, F., Tang, J.-Q., Zhang, Y.-F., Xu, Y. L., & Chi, R.-A. (2017). Selective adsorption and recycle of Cu^{2+} from aqueous solution by modified sugarcane bagasse under dynamic condition. *Environmental Science and Pollution Research*, *24*(10), 9202–9209. https://doi.org/10.1007/s11356-017-8608-2

Das, A., Bar, M., Bar, N., & Das, S. K. (2019). Adsorptive removal of Cr(VI) from aqueous solution: Kinetic, isotherm, thermodynamics, toxicity, scaleup design, and GA modelling. *SN Applied Sciences*, *1*(7), 776. https://doi.org/10.1007/s42452-019-0813-9

Deepali. (2011). Bioremediation of chromium (VI) from textile industry's effluent and contaminated soil using *pseudomonas putida*. *Iranica Journal of Energy & Environment*, *2*(1), 24–31.

Esposito, A., Pagnanelli, F., Lodi, A., Solisio, C., & Vegliò, F. (2001). Biosorption of heavy metals by *Sphaerotilus natans*: An equilibrium study at different pH and biomass concentrations. *Hydrometallurgy*, *60*(2), 129–141. https://doi.org/10.1016/S0304-386X(00)00195-X

Gallo-Cordova, A., Silva-Gordillo, M. del M., Muñoz, G. A., Arboleda-Faini, X., & Streitwieser, D. A. (2017). Comparison of the adsorption capacity of organic compounds present in produced water with commercially obtained walnut shell and residual biomass. *Journal of Environmental Chemical Engineering*, *5*(4), 4041–4050. https://doi.org/10.1016/j.jece.2017.07.052

Ghosh, K., Bar, N., Biswas, A. B., & Das, S. K. (2021). Elimination of crystal violet from synthetic medium by adsorption using unmodified and acid-modified eucalyptus leaves with MPR and GA application. *Sustainable Chemistry and Pharmacy*, *19*, 100370. https://doi.org/10.1016/j.scp.2020.100370

Hasfalina, C. M., Maryam, R. Z., Luqman, C. A., & Rashid, M. (2012). Adsorption of Copper (II) from aqueous medium in fixed-bed column by kenaf fibres. *APCBEE Procedia*, *3*, 255–263. https://doi.org/10.1016/j.apcbee.2012.06.079

Hutchins, R. A. (1973). New method simplifies design of activated-carbon system. *Chemical Engineering*, *80*, 133–138.

Idan, I. J., Abdullah, L. C., Jamil, S. N. A. B. M., Obaid, M. K., & Choong, T. S. Y. (2017). Fixed-bed system for adsorption of anionic acid dyes from binary solute. *BioResources*, *12*(4), 8870–8885.

Kapur, M., & Mondal, M. K. (2016). Design and model parameters estimation for fixed–bed column adsorption of Cu(II) and Ni(II) ions using magnetized saw dust. *Desalination and Water Treatment*, *57*(26), 12192–12203. https://doi.org/10.1080/19443994.2015.1049961

Kuyucak, N., & Volesky, B. (1988). Biosorbents for recovery of metals from industrial solutions. *Biotechnology Letters*, *10*, 137–142. https://doi.org/10.1007/BF01024641

Liu, D., & Sun, D. (2012). Modeling adsorption of Cu(II) using polyaniline-coated sawdust in a fixed-bed column. *Environmental Engineering Science*, *29*(6), 461–465. https://doi.org/10.1089/ees.2010.0435

Maheshwari, U., & Gupta, S. (2016). Removal of Cr(VI) from wastewater using activated neem bark in a fixed-bed column: Interference of other ions and kinetic modelling studies. *Desalination and Water Treatment*, *57*(18), 8514–8525. https://doi.org/10.1080/19443994.2015.1030709

Mandal, A., Bar, N., & Das, S. K. (2020). Phenol removal from wastewater using low-cost natural bioadsorbent neem (Azadirachta indica) leaves: Adsorption study and MLR modelling. *Sustainable Chemistry and Pharmacy*, *17*, 100308. https://doi.org/10.1016/j.scp.2020.100308

Mitra, T., & Das, S. K. (2020). Removal of Cu(II) ions using bio-adsorbents in fixed–Bed continuous bed mode–A comparative study and scale-up design. *Environmental Progress & Sustainable Energy*, *39*(5), e013417. https://doi.org/10.1002/ep.13417

Mitra, T., Bar, N., & Das, S. K. (2019). Rice husk: Green adsorbent for Pb(II) and Cr(VI) removal from aqueous solution–column study and GA–NN modelling. *SN Applied Sciences*, *1*(5), 486. https://doi.org/10.1007/s42452-019-0513-5

Mitra, T., Bar, N., & Das, S. K. (2021). Biosorption of Cu(II) ions from industrial effluents by rice husk: Experiment, statistical and ANN modelling. *Journal of Environmental Engineering and Landscape Management*, *29*(4), 441–448. https://doi.org/10.3846/jeelm.2021.14386

Nag, S., Bar, N., & Das, S. K. (2019). Sustainable bioremadiation of Cd(II) in fixed bed column using green adsorbents: Application of Kinetic models and GA-ANN technique. *Environmental Technology & Innovation*, *13*, 130–145. https://doi.org/10.1016/j.eti.2018.11.007

Nag, S., Bar, N., & Das, S. K. (2020). Cr(VI) removal from aqueous solution using green adsorbents in continuous bed column – statistical and GA-ANN hybrid modelling. *Chemical Engineering Science*, *226*, 115904. https://doi.org/10.1016/j.ces.2020.115904

Ngah, W. S. W., & Hanafiah, M. A. K. M. (2008). Removal of heavy metal ions from wastewater by chemically modified plant wastes as adsorbents: A review. *Bioresource Technology*, *99*(10), 3935–3948. https://doi.org/10.1016/j.biortech.2007.06.011

Nwabanne, J. T., & Igbokwa, P. K. (2012). Adsorption performance of packed bed column for the removal of lead (II) using oil palm fibre. *International Journal of Applied Science and Technology*, *2*(5), 106–115.

Pino, G. H. (2005). *Biosorption of heavy metals using powder of green coconut shell* [Master's Degree dissertation]. Catholic University of Rio de Janeiro, Brazil (in Portuguese).

Pino, G. H., Mesquita, L. M. S. de, Torem, M. L., & Pinto, G. A. S. (2006). Biosorption of heavy metals by powder of green coconut shell. *Separation Science and Technology*, *41*(14), 3141–3153. https://doi.org/10.1080/01496390600851640

Sarkar, S., & Das, S. K. (2016a). Removal of Cr(VI) and Cu(II) ions from aqueous solution by rice husk ash—column studies. *Desalination and Water Treatment*, *57*(43), 20340–20349. https://doi.org/10.1080/19443994.2015.1107754

Sarkar, S., & Das, S. K. (2016b). Removal of hexavalent chromium from aqueous solution using natural adsorbents - column studies. *International Journal of Engineering Research & Technology*, 5(11), 370–377. https://doi.org/10.17577/IJERTV5IS110270

Senthil, P. K., Deepthi, A. S. L. S., Bharani, R., & Rakkesh, G. (2015). Study of adsorption of Cu(II) ions from aqueous solution by surface-modified *Eucalyptus globulus* seeds in a fixed-bed column: Experimental optimization and mathematical modelling. *Research on Chemical Intermediates*, *41*(11), 8681–8698. https://doi.org/10.1007/s11164-015-1921-9

Shahbazi, A., Younesi, H., & Badiei, A. (2013). Batch and fixed-bed column adsorption of Cu(II), Pb(II) and Cd(II) from aqueous solution onto functionalised SBA-15 mesoporous silica. *The Canadian Journal of Chemical Engineering*, *91*(4), 739–750. https://doi.org/10.1002/cjce.21691

Singha, B., & Das, S. K. (2011). Biosorption of Cr(VI) ions from aqueous solutions: Kinetics, equilibrium, thermodynamics and desorption studies. *Colloids and Surfaces B: Biointerfaces*, *84*(1), 221–232. https://doi.org/10.1016/j.colsurfb.2011.01.004

Singha, B., & Das, S. K. (2013). Adsorptive removal of Cu(II) from aqueous solution and industrial effluent using natural/agricultural wastes. *Colloids and Surfaces B: Biointerfaces*, *107*, 97–106. https://doi.org/10.1016/j.colsurfb.2013.01.060

Sivaprakash, B., Rajamohan, N., & Mohamed Sadhik, A. (2010). Batch and column sorption of heavy metal from aqueous solution using a marine alga *Sargassum Tenerrimumint. International Journal of ChemTech Research*, *2*(1), 155–162.

Thomas, H. C. (1944). Heterogeneous ion exchange in a flowing system. *Journal of American Chemical Society*, *66*, 1664–1666. https://doi.org/10.1021/ja01238a017

Wang, F., Yu, J., Zhang, Z., Xu, Y., & Chi, R. (2018). An amino-functionalized ramie stalk-based adsorbent for highly effective Cu^{2+} removal from water: Adsorption performance and mechanism. *Process Safety and Environmental Protection*, *117*, 511–522. https://doi.org/10.1016/j.psep.2018.05.023

Wolborska, A. (1989). Adsorption on activated carbon of *p*-nitrophenol from aqueous solution. *Water Research*, *23*(1), 85–91. https://doi.org/10.1016/0043-1354(89)90066-3

Xavier, A. L. P., Adarme, O. F. H., Furtado, L. M., Ferreira, G. M. D., Silva, L. H. M., Gil, L. F., & Gurgel, L. V. A. (2018). Modeling adsorption of copper(II), cobalt(II) and nickel(II) metal ions from aqueous solution onto a new carboxylated sugarcane bagasse. Part II: Optimization of monocomponent fixed-bed column adsorption. *Journal of Colloid and Interface Science*, *516*, 431–445. https://doi.org/10.1016/j.jcis.2018.01.068

Yahaya, N. K. E. M., Abustan, I., Latiff, M. F. P. M., Bello, O. S., & Ahmad, M. A. (2011). Fixed-bed column study for Cu (II) removal from aqueous solutions using rice husk based activated carbon. *International Journal of Engineering & Technology*, *11*, 186–190.

Yan, G., Viraraghavan, T., & Chem, M. (2001). A new model for heavy metal removal in a biosorption column. *Adsorption Science & Technology*, *19*(1), 25–43. https://doi.org/10.1260/0263617011493953

Yoon, Y. H., & Nelson, J. H. (1984). Application of gas adsorption kinetics I. A theoretical model for respirator cartridge service life. *American Industrial Hygiene Association Journal*, *45*(8), 509–516. https://doi.org/10.1080/15298668491400197